Multifluid description of astrophysical and space plasmas

- Part 1 -

Daniel Gómez[1,2]

(1) Departamento de Física, Fac. Cs. Exactas y Naturales, UBA, Argentina
(2) Instituto de Astronomía y Física del Espacio, UBA-CONICET, Argentina

Giambiagi Lecture Hall

Juan Jose Giambiagi graduated in physics in 1948 at the University of Buenos Aires (Argentina) and received his PhD in 1950.

He was Director of our Physics Department in 1966, and had to leave the University of Buenos Aires and the country during a military coup, after the so-called “night of the long sticks”.

He settled in Brazil and pioneered the development of physics in Latinamerica. He was the Director of the Centro Latinoamericano de Fisica (CLAF) for several years (1986-1994).

He also participated in the early stages of the creation of ICTP in the early 60s and was a member of its Scientific Council from 1987 to 1995.

He made important contributions to dimensional regularization in collaboration with Carlos Bollini.

Magnetic fields in Astrophysics

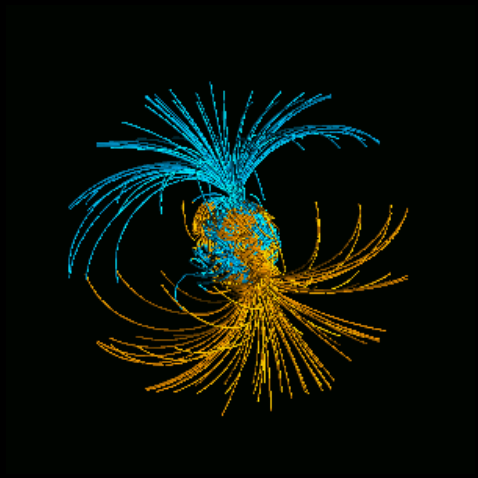

Earth and planets

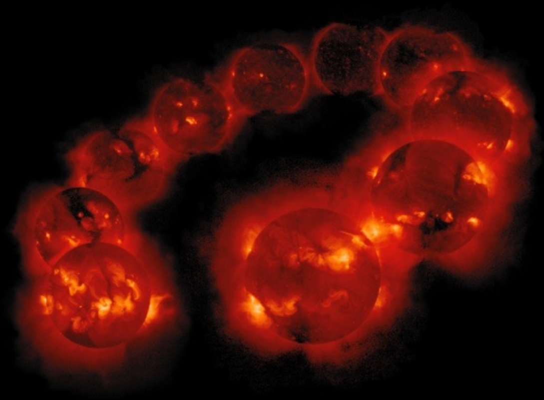

Sun and stars

Interstellar medium

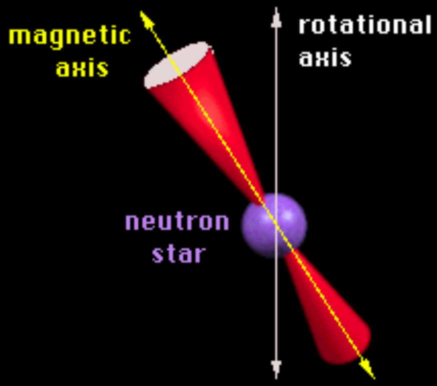

Pulsars

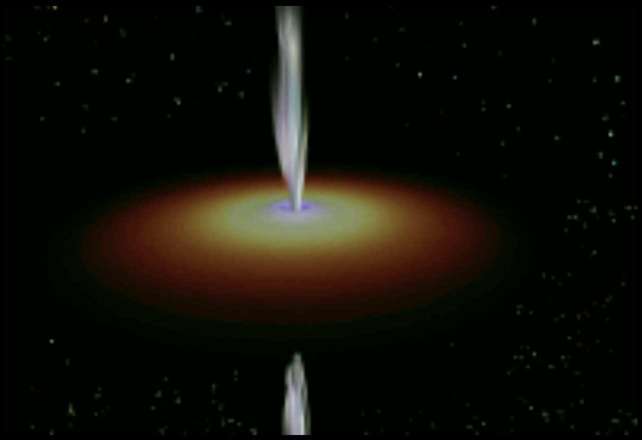

Accretion disks

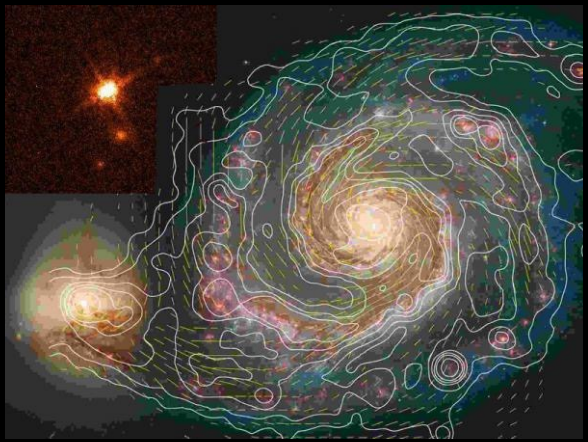

Galaxies

What do we mean by MHD?

➡ It is a fluid-like theoretical description for the dynamics of matter

➡ Baryonic matter in the Universe is mostly hydrogen.

➡ At temperatures above 10^4 K it becomes a hydrogen plasma, i.e. a gas made of protons and electrons

➡ The large scale behavior of this gas can be described through fluidistic equations (Navier-Stokes).

➡ This fluid is made of electrically charged particles and therefore it suffers electric and magnetic forces.

➡ Not only that, these charges are sources of self-consistent electric and magnetic fields. Therefore, the fluid equations will couple to Maxwell's equations.

➡ At small spatial scales (and fast timescales) non-fluid or kinetic effects become non-negligible.

MHD equations

➡ The MHD equations are:

$$\frac{\partial \rho}{\partial t} = -\vec{\nabla} \bullet (\rho \vec{u}) \qquad\qquad p = p_0 \left(\frac{\rho}{\rho_0}\right)^{\gamma}$$

$$\rho \frac{\partial \vec{u}}{\partial t} = -\rho (\vec{u} \bullet \vec{\nabla})\vec{u} - \vec{\nabla} p + \frac{1}{4\pi}(\vec{\nabla} \times \vec{B}) \times \vec{B} + \vec{F}_{ext} + \vec{\nabla} \bullet \overleftrightarrow{\sigma}_{visc}$$

$$\frac{\partial \vec{B}}{\partial t} = \vec{\nabla} \times (\vec{u} \times \vec{B}) + \eta \nabla^2 \vec{B}, \qquad\qquad \vec{\nabla} \bullet \vec{B} = 0$$

which describe the dynamics of the fluid as well as the evolution of the magnetic field.

➡ The induction equation is the result of Ohm's law

$$\vec{E} + \tfrac{1}{c} \vec{u} \times \vec{B} = \frac{1}{\sigma} \vec{J}, \qquad \eta = \frac{c^2}{4\pi\sigma}$$

and Faraday's equation.

MHD equations

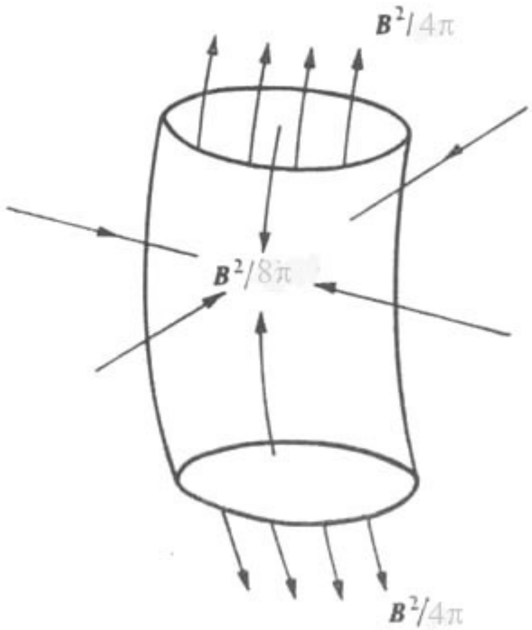

➡ The magnetic force can be split into:

$$\frac{1}{4\pi}(\vec{\nabla}\times B)\times B=\frac{1}{4\pi}(B\cdot\vec{\nabla})B-\vec{\nabla}\left(\frac{B^2}{8\pi}\right)$$

Magnetic pressure
and magnetic tension

➡ In the asymptotic limit of negligible resistivity:

$$\frac{\partial B}{\partial t}=\vec{\nabla}\times(u\times B)$$

Frozen-in condition

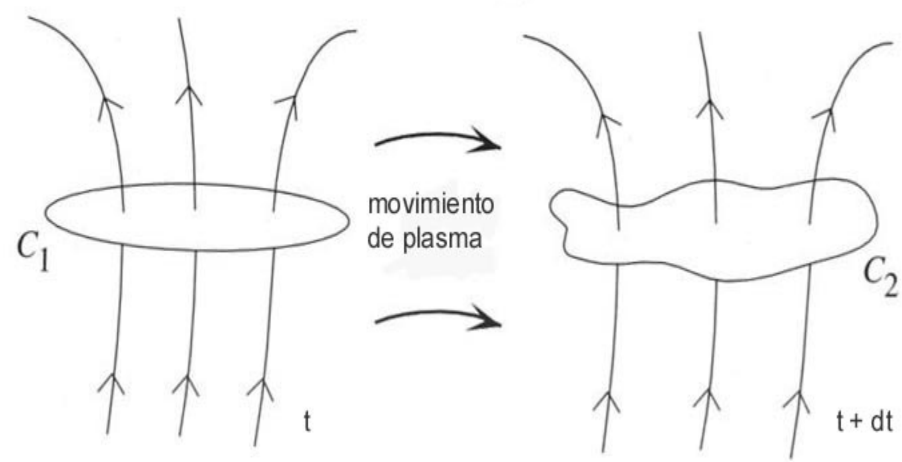

Aplications of MHD

➡ Within this level of description (which is adequate at large spatial scales) there is a variety of important plasma processes that have traditionally been addressed:

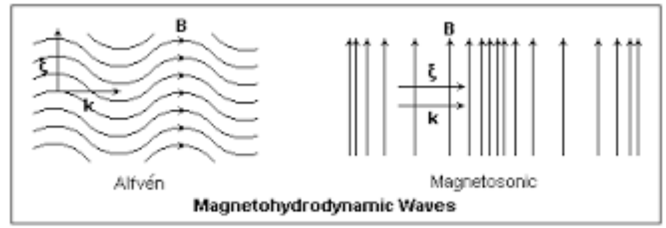

➡ Instabilities, shocks and waves (Alfven and magnetosonic)

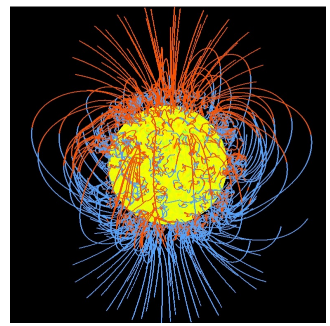

➡ Dynamo mechanisms to generate magnetic fields

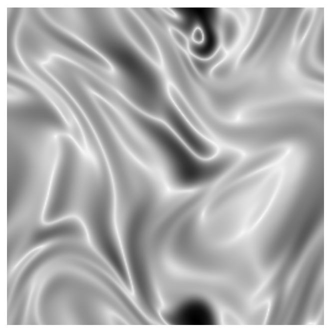

➡ MHD turbulence

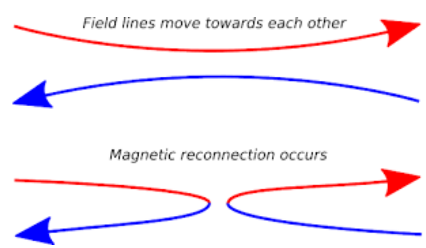

➡ Magnetic reconnection

Simulations

➡ We integrate the MHD equations numerically, using a spectral scheme in all three spatial directions (Gomez, Milano and Dmitruk 2000; also Dmitruk, Gomez & Matthaeus 2003)

➡ We show results from 256x256x256 runs performed in (CAPS), our linux cluster with 80 cores

➡ For the spatial derivatives, we use a pseudo-spectral scheme with 2/3-dealiasing. Spectral codes are well suited for turbulence studies, since they provide exponentially fast convergence.

➡ Time integration is performed with a second order Runge-Kutta scheme.The time step is chosen to satisfy the CFL condition.

caps

Cluster for Astrophysical Plasma Simulations

Fluid turbulence

- Energy cascade
  - energy flux toward high k
  - vortex breakdown

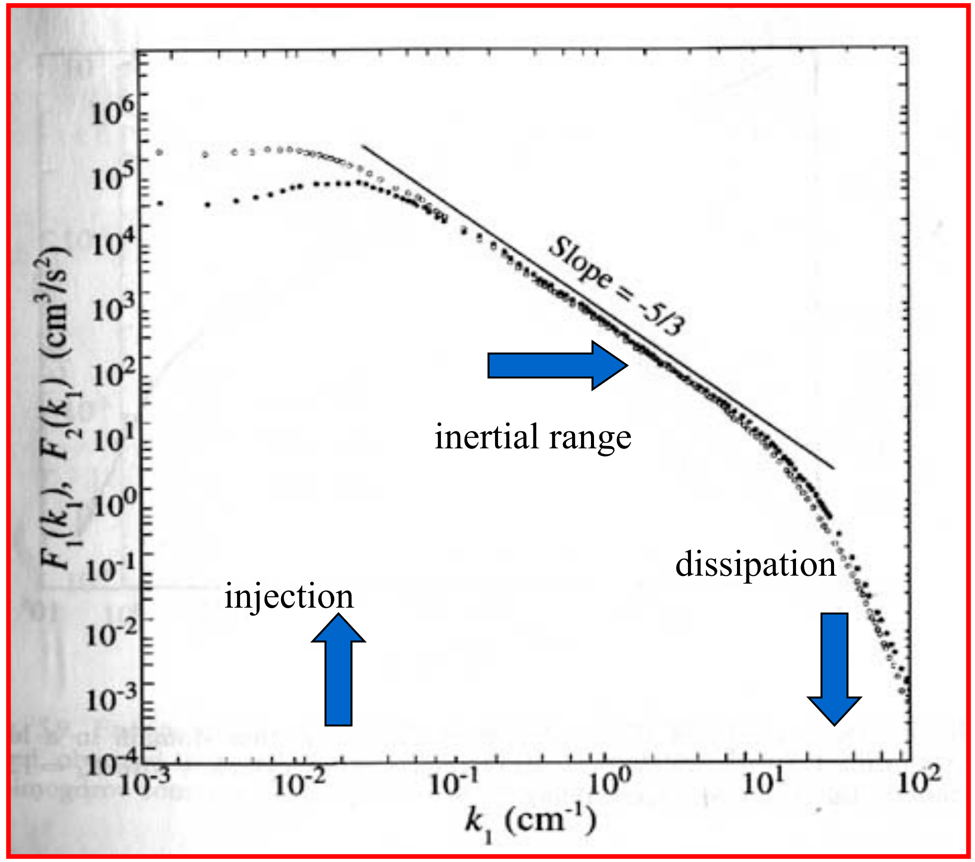

- Scale invariance
  - energy flux in k:

$$\varepsilon_k \approx \frac{u_k^2}{\tau_k}$$

  - energy power spectrum:

$$E_k \approx \frac{u_k^2}{k}$$

$$\tau_k \approx \frac{1}{ku_k}\ ,\ \varepsilon_k \approx \frac{u_k^2}{\tau_k} = const.$$

Therefore

- $$E_k \approx \frac{u_k^2}{k} = \varepsilon^{\frac{2}{3}} k^{-\frac{5}{3}}$$

Kolmogorov spectrum (K41)

MHD-3D dynamos

➡ From mean field theory (Krause & Radler 1980), we know that the turbulent generation of magnetic fields (the **alpha effect**) is proportional to the **kinetic helicity** of the flow. $H = \frac{1}{2}\langle \vec{u} \bullet \vec{\nabla} \times \vec{u} \rangle$

➡ To study this mechanism through direct simulations, we externally drive the flow with a helical force at large scales (an ABC pattern), until a stationary turbulent state is reached (Mininni, Gómez & Mahajan, 2003, ApJ, 587, 472; Mininni, Gómez & Mahajan, 2005, ApJ, 619, 1019)

➡ At that point, a magnetic seed is implanted at small scales and the 3D MHD equations are evolved (Meneguzzi, Frisch & Pouquet 1981).

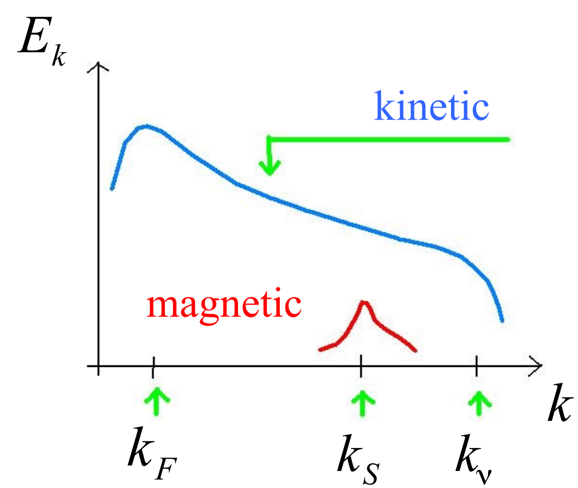

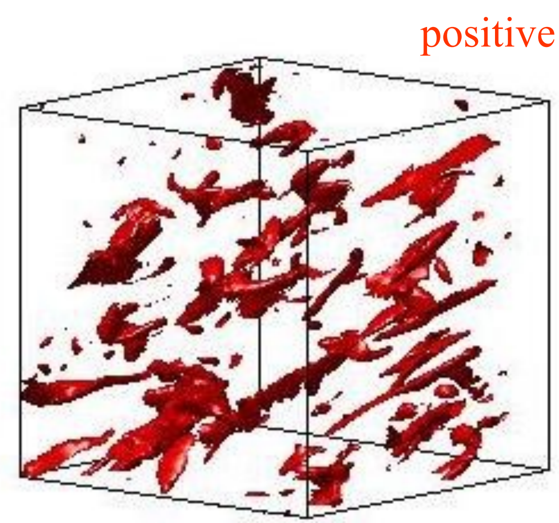

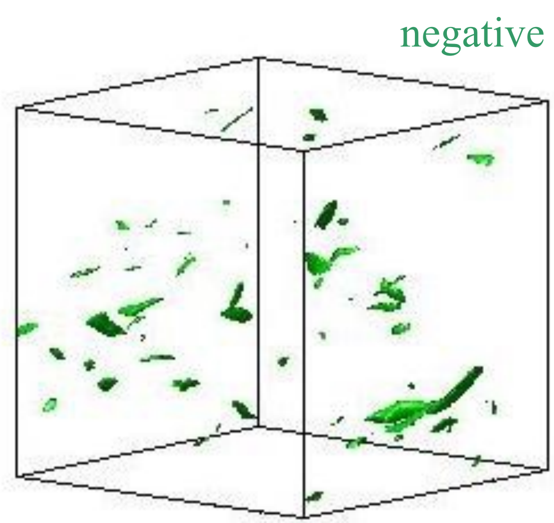

➡ The boxes show the intermittent spatial distribution of positive and negative kinetic helicity H, clearly displaying a net unbalance.

Energy power-spectra

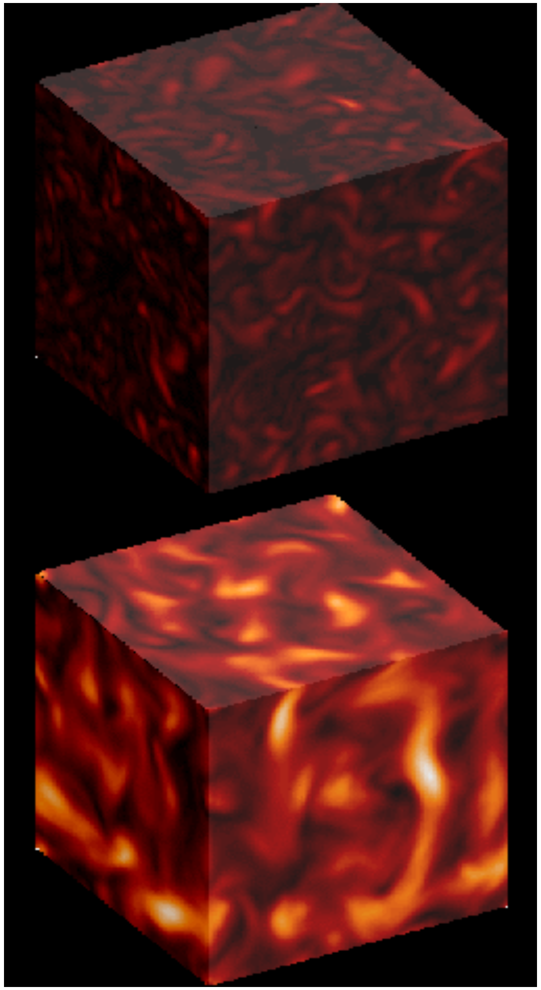

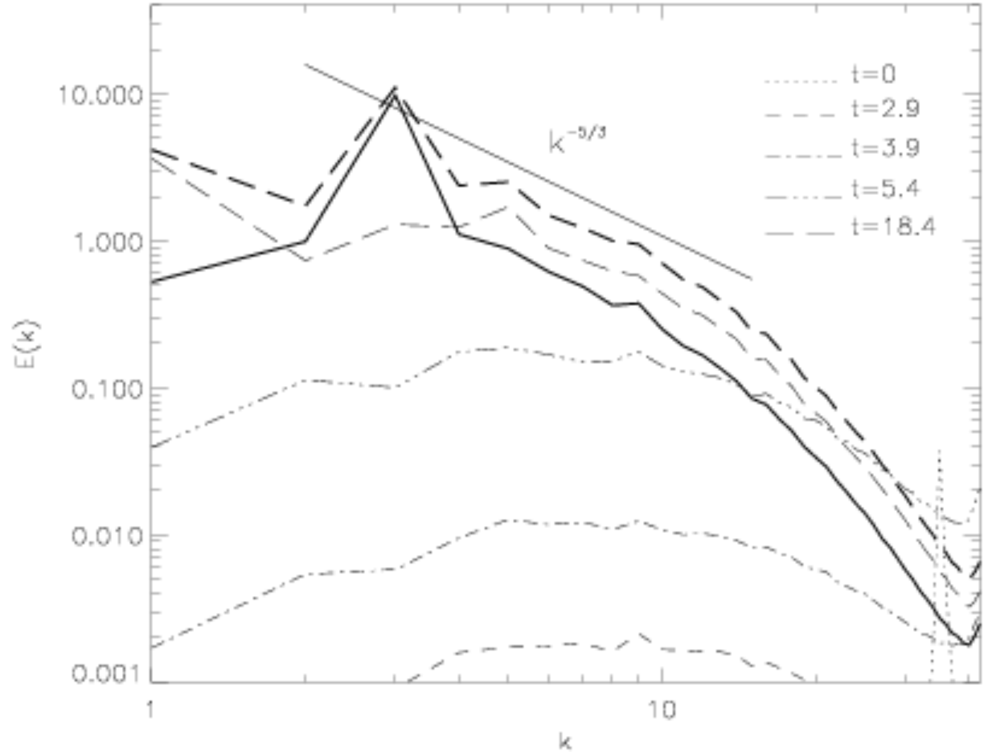

➡ The power spectrum of magnetic energy grows in time until it reaches equipartition at each scale (Brandenburg et al. 2003).

➡ The Kolmogorov slope is also displayed for reference.

➡ The full line is the kinetic energy power spectrum and the dotted line is the total energy.

Energy power-spectra

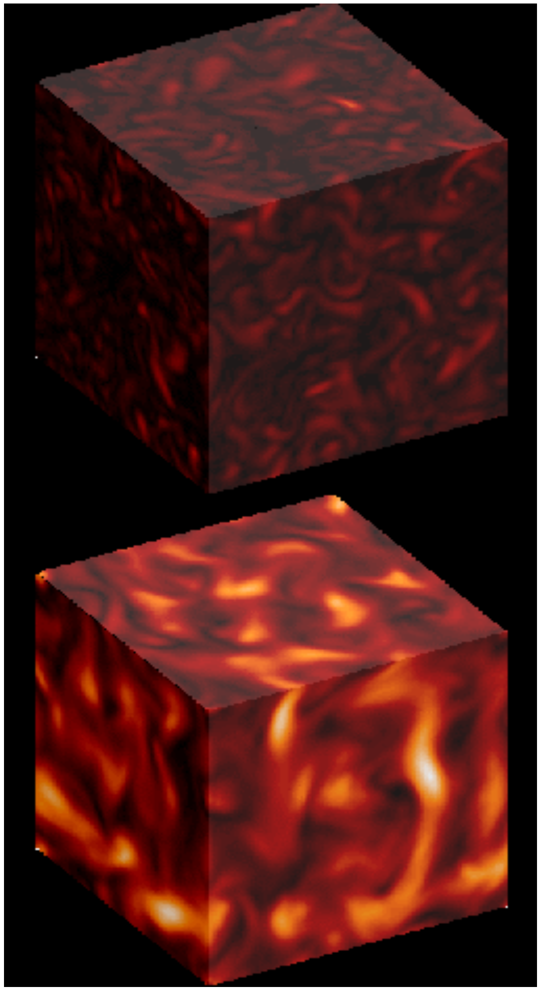

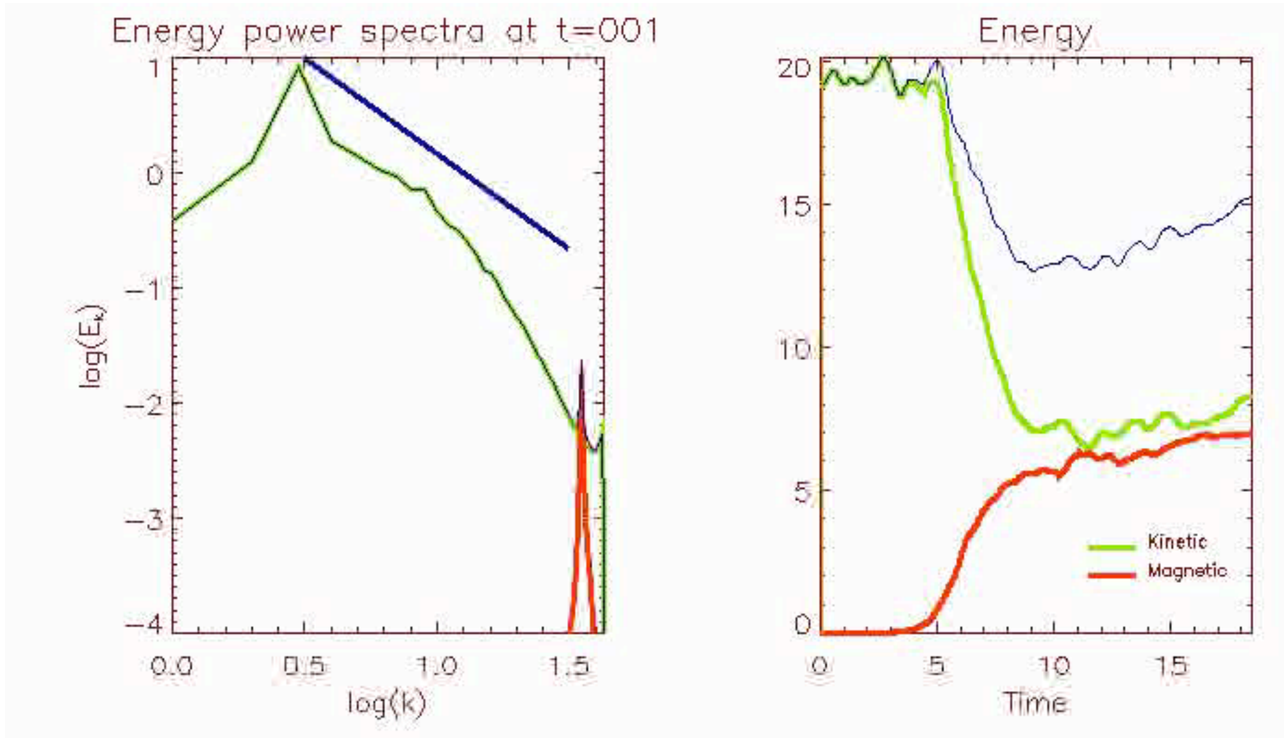

➡ The power spectrum of magnetic energy grows in time until it reaches equipartition at each scale (Brandenburg et al. 2003).

➡ The Kolmogorov slope is also displayed for reference.

➡ The green line is the kinetic energy power spectrum and the red line is the magnetic energy.

Turbulent dynamos

➡ The image on the right shows the spatial distribution of magnetic energy.

➡ The image below shows an initial exponential growth stage (kinematic dynamo) for the total magnetic energy. At later times it saturates when it reaches approximate equipartition with the total kinetic energy of the turbulent flow.

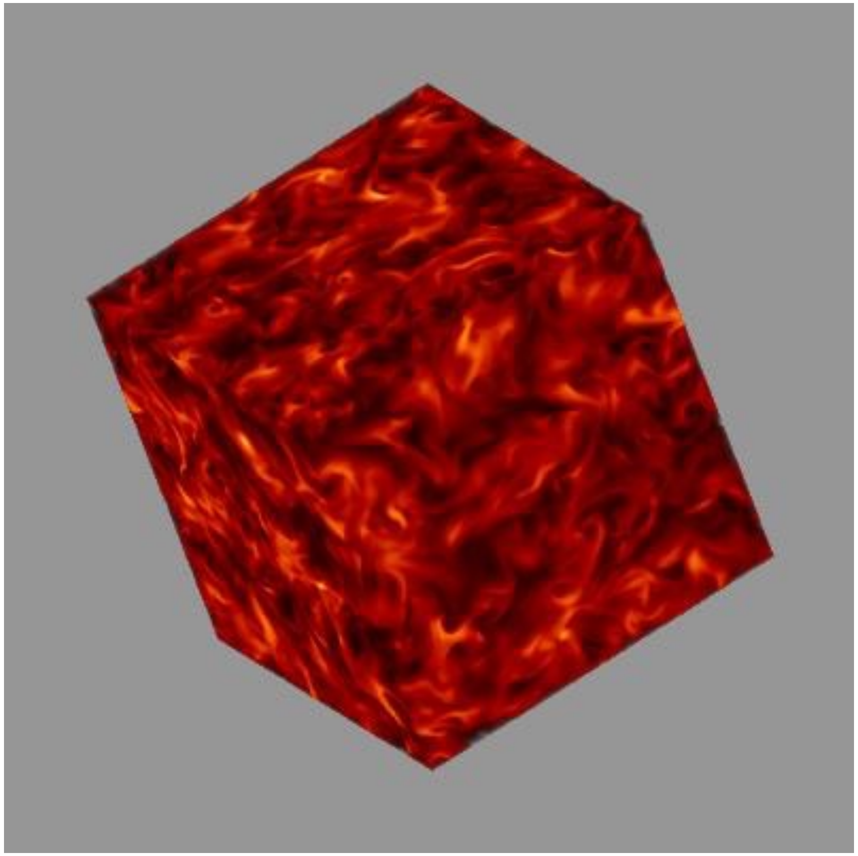

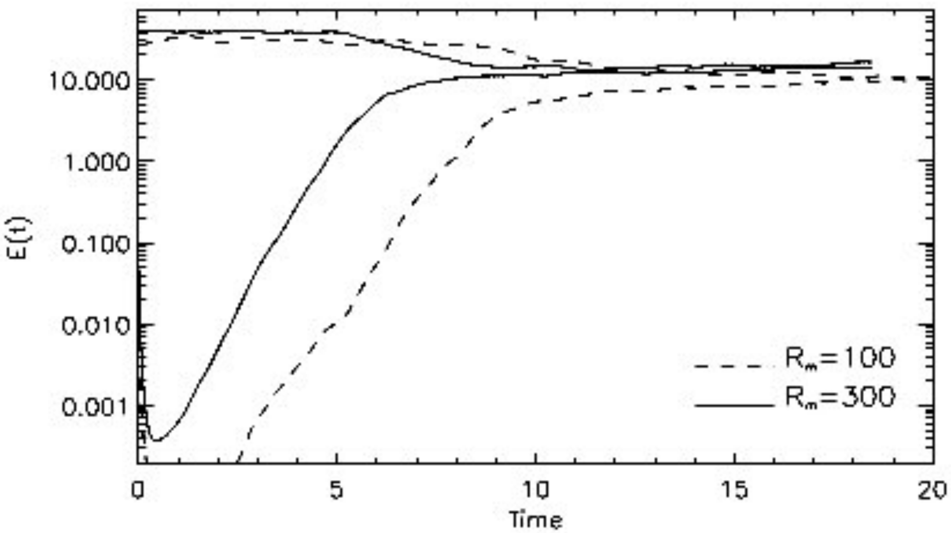

➡ As predicted by MFT (Steenbeck et al. 1966), kinematic helicity (H) at the microscale produces magnetic field at macroscopic scales (large-scale dynamos).

Force-free equilibria

➡ When forcing is applied at intermediate scales, an accumulation of magnetic energy is observed at the largest scales.

➡ This behavior is caused by the inverse cascade of magnetic helicity.

➡ The magnetic field at large scales is approximately force-free, i.e.

$$\vec{\nabla} \times \vec{B} \;//\; \vec{B}$$

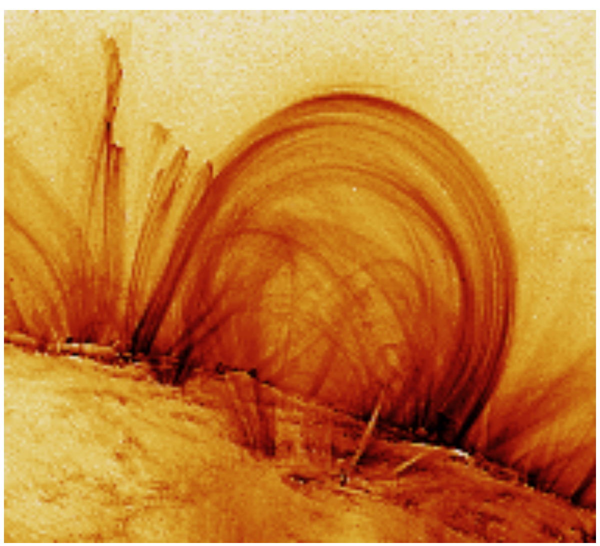

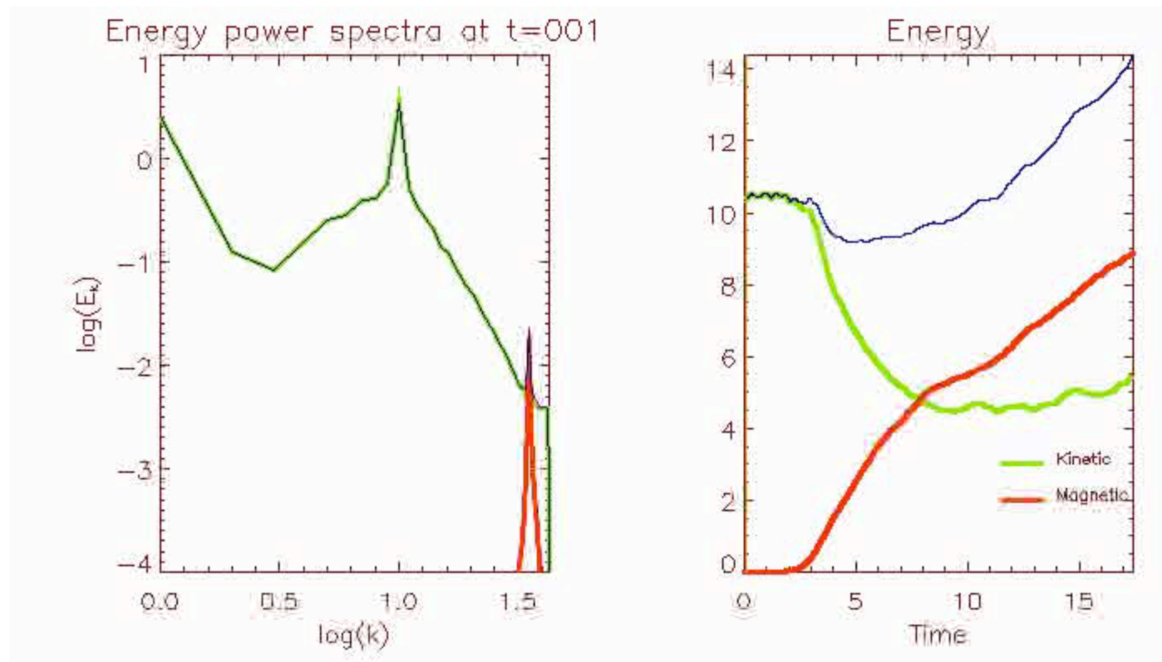

➡ Small scales, however, are consistent with a strongly turbulent MHD regime.

➡ This configuration can be representative of active regions of the solar corona, which are approximately force-free at large scales and at the same time are being heated by a strong MHD turbulence at smaller scales (Gómez & F.Fontán 1988)

Fluid equations for multi-species plasmas

➡ For each species s we have (Goldston & Rutherford 1995):

- Mass conservation

$$\frac{\partial n_s}{\partial t} + \vec{\nabla} \cdot (n_s \vec{U}_s) = 0$$

- Equation of motion

$$m_s n_s \frac{d\vec{U}_s}{dt} = q_s n_s (\vec{E} + \frac{1}{c}\vec{U}_s \times \vec{B}) - \vec{\nabla} p_s + \vec{\nabla} \bullet \vec{\vec{\sigma}}_s + \sum_{s'} \vec{R}_{ss'}$$

- Momentum exchange rate

$$\vec{R}_{ss'} = -m_s n_s \upsilon_{ss'} (\vec{U}_s - \vec{U}_{s'})$$

➡ These moving charges act as sources for electric and magnetic fields:

- Charge density

$$\rho_c = \sum_s q_s n_s \approx 0$$

- Electric current density

$$\vec{J} = \frac{c}{4\pi} \vec{\nabla} \times \vec{B} = \sum_s q_s n_s \vec{U}_s$$

for non-relativistic plasmas

Small scales: two-fluid MHD

➡ The dimensionless version, for a length scale L_0 , density n_0 and Alfven speed $v_A = B_0 / \sqrt{4\pi m_i n_0}$

$$\frac{d\vec{U}_i}{dt} = \frac{1}{\varepsilon}(\vec{E} + \vec{U}_i \times \vec{B}) - \frac{\beta}{n}\vec{\nabla} p_i - \frac{\eta}{\varepsilon n}\vec{J}$$

$$\frac{m_e}{m_i}\frac{d\vec{U}_e}{dt} = -\frac{1}{\varepsilon}(\vec{E} + \vec{U}_e \times \vec{B}) - \frac{\beta}{n}\vec{\nabla} p_e + \frac{\eta}{\varepsilon n}\vec{J}$$

where $\vec{J} = \vec{\nabla} \times \vec{B} = \frac{n}{\varepsilon}(\vec{U}_i - \vec{U}_e)$

➡ We define the Hall parameter $\varepsilon = \frac{c}{\omega_{pi} L_0}$

as well as the plasma *beta* $\beta = \frac{p_0}{m_i n_0 v_A^2}$ and the electric resistivity $\eta = \frac{c^2 \nu_{ie}}{\omega_{pi}^2 L_0 v_A}$

➡ Adding these two equations yields:

$$\frac{d\vec{U}}{dt} = (\vec{\nabla} \times \vec{B}) \times (\vec{B} + \varepsilon_e^2 \vec{\nabla} \times \vec{J}) - \vec{\nabla} p$$

where $\vec{U} = \frac{m_i \vec{U}_i + m_e \vec{U}_e}{m_i + m_e}$

$$\varepsilon_e = \sqrt{\frac{m_e}{m_i}}\,\varepsilon = \frac{c}{\omega_{pe} L_0}$$

and $p = p_i + p_e$

Generalized Ohm's law

- Note that the equation of motion for electrons is also Ohm's law

$$\mu \frac{d\vec{U}_e}{dt} = -\frac{1}{\epsilon}(\vec{E} + \vec{U}_e \times \vec{B}) - \frac{\beta}{n}\vec{\nabla} p_e + \frac{\eta}{n\epsilon}\vec{J}$$

where $\mu = \frac{m_e}{m_i} \ll 1$

- Considering that

$$\vec{U} = \frac{m_e\vec{U}_e + m_i\vec{U}_i}{m_e + m_i}$$

$$\vec{J} = n(\vec{U}_i - \vec{U}_e)$$

$$n = 1 \quad \text{(incompressible)}$$

$$\Rightarrow \quad \vec{U}_i = \vec{U} + \mu\epsilon\vec{J}$$

$$\vec{U}_e = \vec{U} - (1-\mu)\epsilon\vec{J}$$

- In the limit of massless electrons (i.e. $\mu \to 0$)

$$0 = -(\vec{E} + (\vec{U} - \epsilon\vec{J}) \times \vec{B}) - \beta\epsilon\vec{\nabla} p_e + \eta\vec{J}$$

also known as the generalized Ohm's law

- At large scales, much larger than the ion inertial length (i.e. $\epsilon \to 0$), it reduces to

$$E + \vec{U} \times \vec{B} = \eta\vec{J}$$

Ideal invariants in multi-fluid plasmas

- For each species s in the incompressible and ideal limit

$$m_s n_s\left(\partial_t \vec{U}_s - \vec{U}_s \times \vec{W}_s\right) = q_s n_s\left(\vec{E} + \frac{1}{c}\vec{U}_s \times \vec{B}\right) - \vec{\nabla}\left(p_s + m_s n_s \frac{U_s^2}{2}\right)$$

- Using that $\vec{J} = \frac{c}{4\pi}\vec{\nabla}\times\vec{B} = \sum_s q_s n_s \vec{U}_s$ and $E = -\frac{1}{c}\partial_t \vec{A} - \vec{\nabla}\phi$

we can readily show that energy is an ideal invariant, where

$$E = \int d^3r \left(\sum_s m_s n_s \frac{U_s^2}{2} + \frac{B^2}{8\Pi}\right)$$

- We also have a helicity per species which is conserved, where

$$H_s = \int d^3r \left(\vec{A} + \frac{cm_s}{q_s}\vec{U}_s\right) \bullet \left(\vec{B} + \frac{cm_s}{q_s}\vec{W}_s\right)$$

Normal modes in 2F-HMHD

- If we linearize our equations around an equilibrium characterized by a uniform magnetic field we obtain, in the incompresible case, the following dispersion relation:

$$\left(\frac{\omega}{\vec{k}\bullet\vec{B}_0}\right)^2 \pm \frac{k\varepsilon}{1+\varepsilon_e^2 k^2}\left(\frac{\omega}{\vec{k}\bullet\vec{B}_0}\right) - \frac{1}{1+\varepsilon_e^2 k^2} = 0$$

- Asymptotically, at very large k, we have two branches

$$\omega \xrightarrow[k\to\infty]{} \omega_{ce}\cos\theta$$

$$\omega \xrightarrow[k\to\infty]{} \omega_{ci}\cos\theta$$

while for very small k, both branches simply become Alfven modes, i.e.

$$\omega \xrightarrow[k\to 0]{} k\cos\theta$$

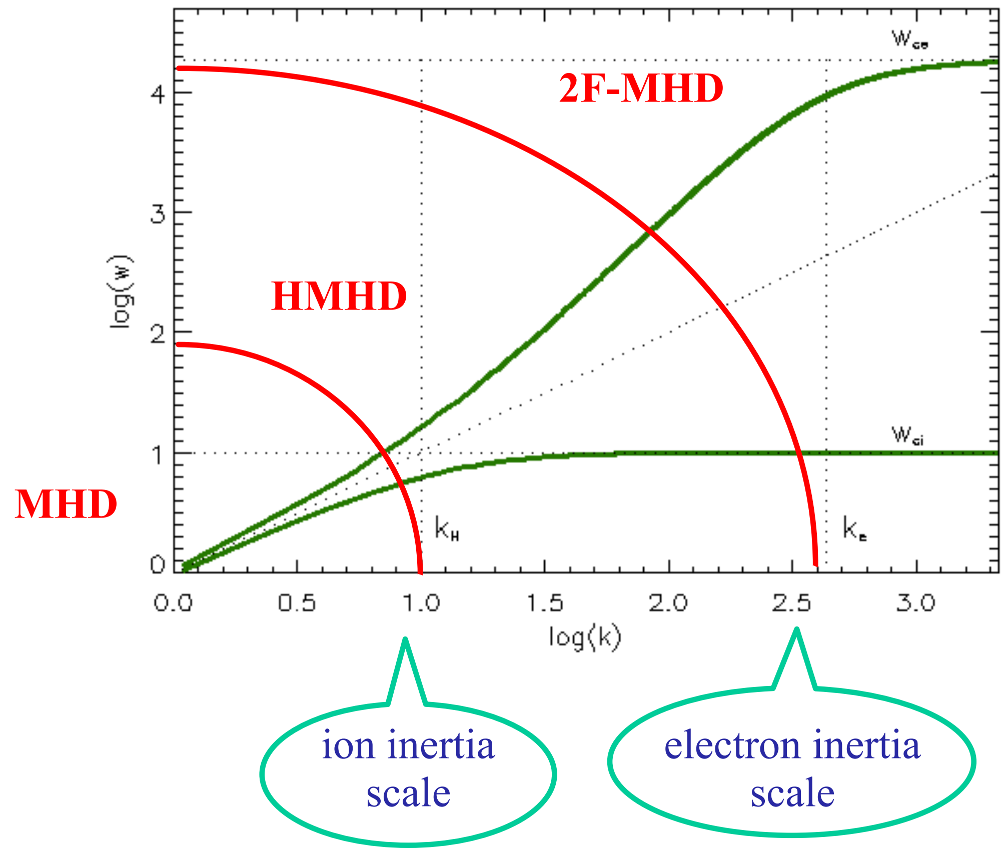

- Different approximations, just as one-fluid MHD, Hall-MHD and electron-inertia MHD can clearly be identified in this diagram.

Some applications

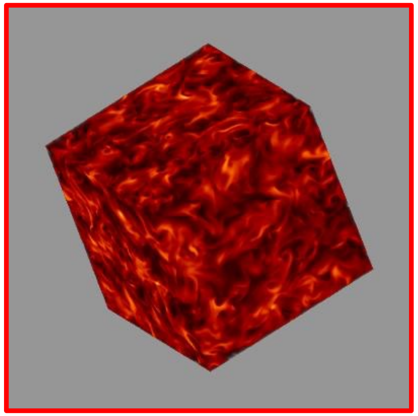

MHD

RMHD heating of solar coronal loops (Dmitruk & Gomez 1997, 1999)

Kelvin-Helmholtz instability in the solar corona (Gomez, DeLuca & Mininni 2016)

Hall-MHD

3D HMHD turbulent dynamos. (Mininni, Gomez & Mahajan 2003, 2005; Gomez, Dmitruk & Mininni 2010)

2.5 D HMHD reconnection at Earth magnetopause (Morales, Dasso & Gomez 2005, 2006)

RHMHD turbulence in the solar wind (Martin, Dmitruk & Gomez 2010, 2012)

Hall MRI in accretion disks (Bejarano, Gomez & Brandenburg 2011)

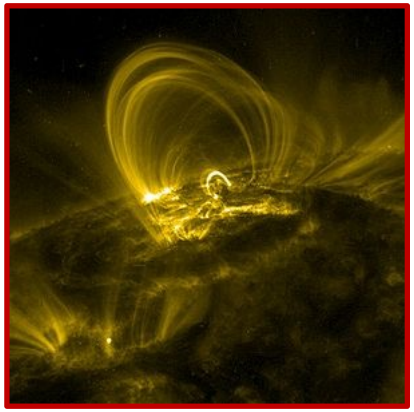

Electron inertia

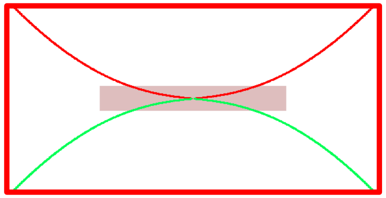

1D model of perpendicular shocks (Gomez et al. 2021).

Two-fluid turbulence in the solar wind (Andres et al. 2014, 2016).

Fast reconnection in 2.5 D (Andres, Dmitruk & Gomez 2014, 2016).

Conclusions

- Today we presented the **MHD equations** as a valid description of the large-scale behavior of astrophysical plasmas.

- As an example, we numerically show a **turbulent dynamo** in action. An initial magnetic seed grows to equipartion with kinetic energy, provided that the flow is helical.

- We also introduced the **two-fluid description** as an extended version of MHD that goes beyond the ion and even the electron inertial lengths.

- In the next lecture, we will explore various applications of this extended MHD, such as shock formation, turbulence and magnetic reconnection.

Simulations: spatial integration

➢ We focus on Fourier-Galerkin methods. Let us illustrate on Burgers equation

$$\partial_t u + u \partial_x u = \nu \, \partial_{xx} u$$

for u(x,t) on the interval $0 \le x < 2\pi$ assuming periodic boundary conditions and the initial condition $u(x,0) = u_0(x)$

➢ We expand in a <u>truncated</u> Fourier expansion $\Longrightarrow$ $u^N(x,t) = \sum_{k=-N/2}^{N/2} u_k(t)\, e^{ikx}$

➢ Demanding zero projection of the solution u(x,t) on the truncated Fourier space

$$\partial_t u_k = -(u \partial_x u)_k - \nu\, k^2\, u_k \quad , \quad (u \partial_x u)_k = \sum_{l+m=k} i m u_l u_m$$

➢ This truncated expansion $u^N(x,t)$ converges exponentially fast to the exact solution as $N \to \infty$

However, it is computationally very demanding, it involves $O(N^2)$ operations.

Simulations: spatial integration

➢ The FFT algorithm yields the discrete set $\{\hat{u}_k\}$ from the set $\{u(x_j)\}$ after $O(N \log N)$ floating point operations.

$$\left\{u(x_j)\,,\, x_j = \frac{2\pi}{N} j\,,\, j = 0,\ldots,N-1\right\} \quad \overrightarrow{FFT} \quad \left\{\hat{u}_k\,,\, k = -N/2+1,\ldots,N/2\right\}$$

➢ The strategy of computing spatial derivatives in Fourier space and nonlinear terms in physical space, is known as pseudo-spectral, i.e.

$$\partial_t u_k = -(u\partial_x u)_k - \nu k^2 u_k \quad , \quad (u\partial_x u)_k = FFT(FFT^{-1}(u_k)\, FFT^{-1}(iku_k))$$

➢ The relation between discrete Fourier coefficients $\{\hat{u}_k\}$ and the continuous ones is

$$\hat{u}_k = u_k + \sum_{m\neq 0} u_{k+Nm}$$

➢ This sum causes a spurious effect known as aliasing when computing nonlinear terms. Aliasing effects can be suppressed by applying the "two-thirds rule", i.e.

$$\hat{u}_k = 0 \quad , \quad \forall \quad |k| \geq N/3$$

Simulations: temporal integration

➢ We advance the solution through discrete time steps $\Longrightarrow$ $t_i = i\Delta t$

➢ In compact notation, if $\dfrac{dU}{dt} = F(U,t)$

where F is a nonlinear and spatial differential operator, we use a second order Runge-Kutta scheme.

➢ We first advance half a step $\Longrightarrow$ $U^{i+\frac{1}{2}} = U^i + \dfrac{\Delta t}{2} F(U^i, t_i)$

and use $U^{i+\frac{1}{2}}$ to jump the whole step $\Longrightarrow$ $U^{i+1} = U^i + \Delta t\, F(U^{i+\frac{1}{2}}, t_{i+\frac{1}{2}})$

➢ This is second order accurate (i.e. $O((\Delta t)^2)$). The size of the step is limited by

the CFL condition, i.e $\Delta t \leq \Delta x / u_0$ for $\partial_t u = u_0\, \partial_x u$